eprints@whiterose.ac.uk
https://eprints.whiterose.ac.uk/

Diode Laser Welding of Stainless Steel 304L

J. A. Alcock[a, b, 1]

B. Baufeld[a]

[a]Nuclear AMRC, University of Sheffield, Brunel Way, Rotherham, S60 5WG, UK

[b]Mechanical Engineering, Sheffield Hallam University, City Campus, Howard Street, Sheffield S1 1WB, UK

Corrospending author: B. Baufeld, b.baufeld@namrc.co.uk, Telefon: +44 (0)114 222 9919

Abstract

The feasibility to achieve deep penetration welding of stainless steel utilising a 15 kW laserline® diode laser has been studied. This was approached by first characterising the properties of melt run welds on stainless steel 304L plates and then transferring the gained knowledge to perform the butt welds.

The results from the melt run analysis indicated that there was an increase in penetration and weld width with heat input, i. e. with either increasing the laser power (9 to 15 kW) or decreasing the welding velocity (3 m/min to 1 m/min). Melt run penetrations up to 12 mm were achieved. The increased welding velocity was shown to reduce the solidification grain and subgrain size. Cracks along the weld centreline were observed at the higher heat inputs and sinking at the crowns at the lower. Good melt run welds were obtained at laser powers of 9 to 13 kW and a welding velocity of 1.5 m/min.

Butt welding of 10 mm thick plates was successfully achieved with full penetration along the length of the weld at a laser power of 12 kW and a welding velocity of 1.5 m/min. The weld properties were comparable to the corresponding melt run welds using a similar parameter set of laser power and welding velocity. No detrimental subsurface defects were recorded with only the presence of a negligible amount of porosity. Oxidisation on the surface of the cap and sinking towards the end of the weld run was observed.

It was demonstrated that high powered diode lasers are capable of deep penetration welding. Keyhole mode welding was achieved and the weld properties are comparable to that of other high energy density welding processes. For welding of plates in the 10 mm thickness range, the results suggested that the more economic high power diode lasers may become a competitor to different laser beam systems which may be more expensive in both procurement and operation.

---

[1]present address: Mechanical Engineering, Sheffield Hallam University, City Campus, Howard Street, Sheffield S1 1WB, UK, jack.a.alcock@gmail.com

Introduction

Laser welding is now a common fusion process and is widely applied in industry for a great variety of materials and products. In the following only few examples are listed. Early examples for industrial applications were given by Ready (1997). Dausinger (2000) described industrial laser welding of aluminium. Henderson et al. (2004) illustrated welding practices for industrial gas turbine applications of nickel based alloys. The laser welding of steel power trains was exemplified by Mootz (2016). As Neumann (2016) has explained traditionally CO_2 and ND:YAG lasers were used for industrial laser welding but the tremendous advances in power, beam quality and reliability lead to the increased introduction of solid state lasers such as fibre and disc lasers. These lasers exhibit excellent beam quality and they have the potential to replace CO_2 and ND:YAG lasers in many industrial manufacturing applications.

In comparison to fibre and disc lasers, diode lasers are not usually considered suitable for deep penetration welding, since it is widely assumed that the inferior beam quality of diode lasers excludes this technology for fusion welding. However, in recent years the beam quality of diode lasers has improved significantly and nowadays high power diode lasers up to 20 kW (and according to Ullmann (2016) in near future up to 40 kW) are available. It is now time to evaluate whether the potential technological disadvantages of diode lasers could be counterbalanced by the economic advantages they have. As specified in the following the diode laser technology exhibits significant lower operating costs and less capital investments over other laser types. As Ullmann (2014) has highlighted the electrical efficiency of modern diode lasers of at least 40% is much greater compared to other technologies, reducing the operating cost considerably. Parker (2010) has stated that this goes in line with the reduction of the carbon footprint of the system. Diode laser systems usually occupy a much smaller footprint due to the simpler construction, compact design and the reduced amount of cooling required. Consequently capital investment for a diode laser system is typically lower. A prospective additional technological benefit of diode lasers for welding applications is the shorter wavelength compared to other laser technologies, potentially reducing the problems associated with welding highly reflective materials such as aluminium and stainless steel.

Austenitic stainless steel 304L investigated in the present work is commonly used to manufacture nuclear components including reactor vessels and piping systems in pressurized water reactors (PWR) as described by De Baglion and Mendez (2010)This material is frequently selected because of its corrosion resistant properties and good weldability. Bush (1990) highlights the resistance to erosion-corrosion of this stainless steel. There is usually

2

no requirement for pre- or post-weld heat treatment as, unlike low carbon steel alloys, a martensitic structure does not form in the HAZ. The low carbon grade is preferable in the nuclear industry because of the better intergranular stress corrosion cracking resistance.

It has been shown that deep penetration autogenous laser welding of 304L plates is feasible. Yan et al. (2010) have reported laser welding of 3 mm thick 304 stainless steel plates using a 5 kW CO_2 laser. Buddu et al. (2015) have performed 8 mm thick welds using a 3.5 kW CO_2 laser. Zhang et al. (2014) have achieved 12 mm thick welds applying a 10 kW fibre laser.

The main goal of this paper is report the capability of a high power diode laser in welding type 304L stainless steel. The influence of variations of laser power, P, and welding velocity, v, on the weld was studied for melt runs of 15 mm thick plates and for fusion butt welds of 10 mm thick plates.

Experimental set-up

The work was performed utilising a 15 kW laserline® diode laser (wave length 950 to 1030 nm), a laserline® welding head OTS2, and a 20 m long HIGHYAG® glass fibre with a 1.0 mm core diameter. The manipulation of the welding head was provided by a KUKA® robot achieving downhand welding on horizontal test coupons. Baufeld et al. (2014) and Baufeld and Lawler (2016) give more details of the set-up. The laser beam was tilted at an angle of 15° to the work surface resulting in a leading weld spot in order to prevent damage of the optics by laser reflections.

This paper reports about melt runs and autogenous butt welds. In both cases the weld crown shielding setup consisted of argon fed to the front and back of the melt pool through copper pipes (Figure 1). In the case of the butt welding additional shielding of the root was applied using a purge box flooded with argon. A cross jet of air at the optics was introduced in order to prevent weld spatter damaging the optics and other equipment.

Figure 1 Set-up for melt runs

A clear understanding of the laser beam and potential changes over time is essential for reliable and repetitive welding. Therefore prior to welding, caustic and power measurements were carried out using the Primes® analysis tools FocusMonitor FM120 and PowerMonitor PM100.

Each of the welds was put through various testing methods to characterise the weld properties in relation to the power P and welding velocity v. This included visual inspection of the weld crowns and roots, measuring the width and any surface discontinuities. The samples were then cross sectioned and analysed in the as-polished condition for subsurface defects before being etched (electrolytically at 10 V in 10% oxalic acid) to reveal the microstructure within the fusion zone (FZ) and heat affected zone (HAZ). Microscopy was carried out on the samples using both optical and scanning electron microscope (SEM) techniques. Measurements of the solidification grain and subgrain sizes were performed as well as micro Vickers hardness measurements.

Material

Stainless steel 304L plates were used for all of the welding experiments. The geometries were 300 mm x 300 mm x 15 mm in the case of the melt runs and 300 mm x 150 mm x 10 mm in the case of the butt welds. The composition of the plates was slightly different for the two geometries and is given in Table 1.

4

Table 1 Composition of the Stainless Steel 304L plates used for the melt run and the butt welding trials in wt.% according to the certificates from the suppliers Aperam and Acroni.

Element	C %	Si %	Mn %	P %	S %	Cr %	Ni %	N %	Fe %
min	-	-	-	-	-	18.00	8.00	-	-
max	0.030	0.75	2.00	0.045	0.030	20.00	12.00	0.100	-
Melt runs	0.025	0.36	1.83	0.030	0.023	18.00	8.14	0.090	Bal
Butt Weld	0.022	0.47	1.46	0.030	0.002	18.06	8.03	0.070	Bal

Results

Beam Analysis

Caustic measurements (39 measurement planes over a distance of 15 mm) have been performed at different laser powers from 1 kW to 15 kW. Beam parameters such as focus shift, Rayleigh length and focus diameter have been determined. The focus length of the optics was 129 mm, which shifted with increasing power by less than 1 mm (Figure 2). The focus diameter d and Raleigh length have decreased slightly (Figure 3) for an increase of the laser power from 1 to 15 kW.
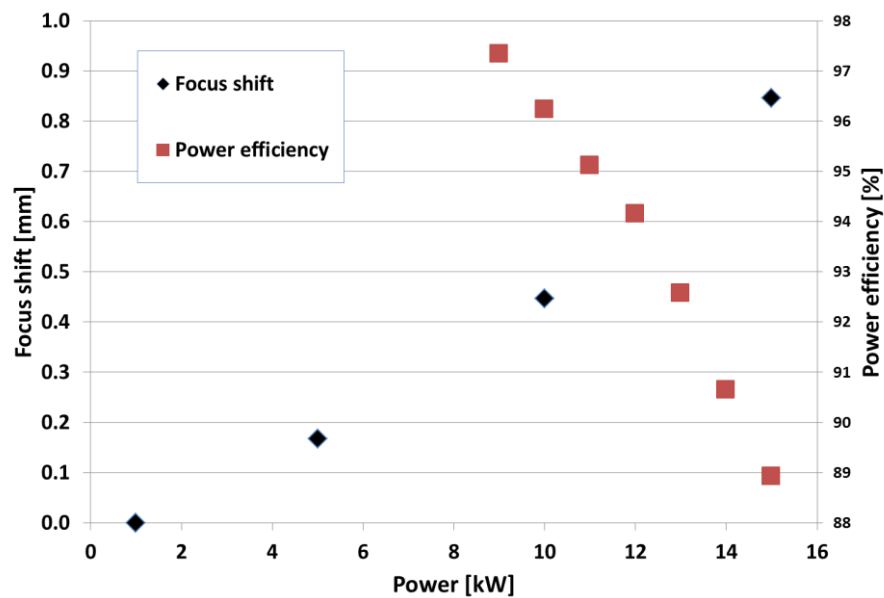

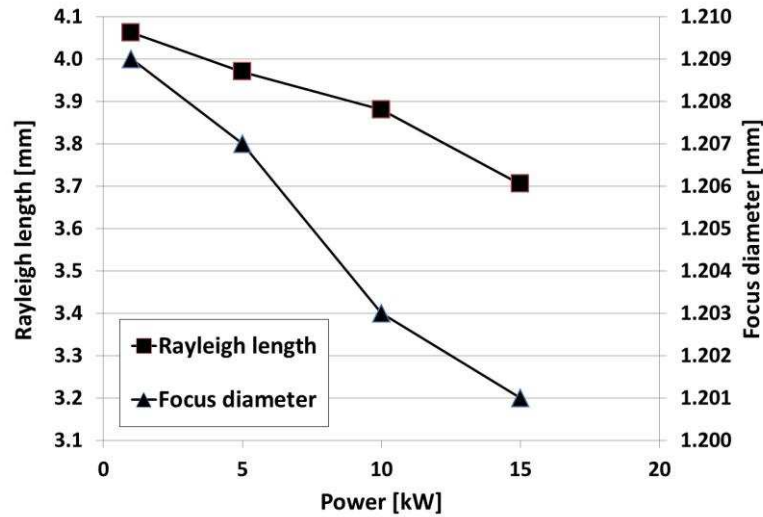**Figure 2 Focus shift and power efficiency in dependence of the laser power**

Figure 3 Rayleigh length and focus diameter of the beam in dependence of the laser power

The laser power available after passing the 20 m fibre and the welding optics have been measured for different set values of laser power from 9 to 15. It was observed that the power efficiency, which is the quotient of actual value and the set value has decreased continuously from about 97 % at 9 kW to 89 % at 15 kW (Figure 2).

Results of melt runs

64 melt runs were performed with a variation of laser power, P, from 9 to 15 kW and the welding velocity, v, from 1.0 to 3.0 m/min. The net heat input, H_{net} (also called line energy) is defined as:

Equation 1

$$H_{net} = \frac{P}{v}$$

The variation of laser power and welding velocity translates to a heat input variation from 189 to 900 J/mm. At low welding velocities a large amount of spatter was created which generally reduced with increasing welding velocity. The width of the weld crowns was relatively large, increasing with the heat input (Figure 4), i. e. it increased with laser power and decreases with welding speed.
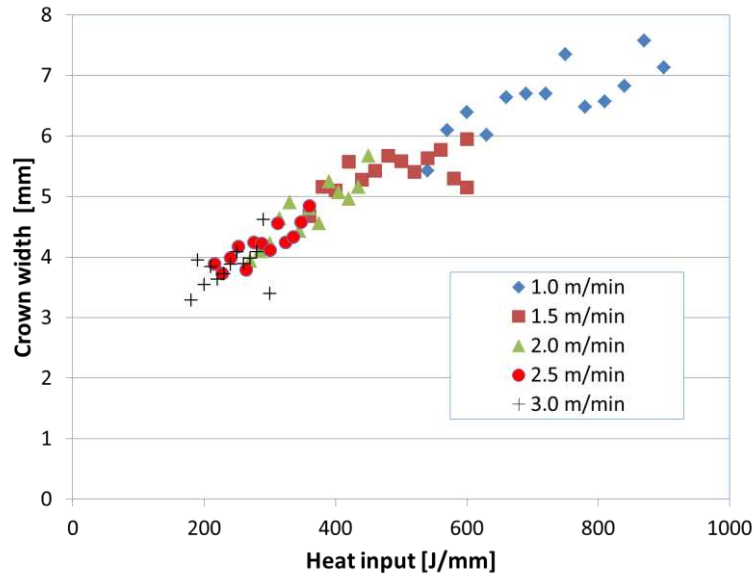
6

Figure 4 Weld crown width in dependence on the heat input for laser power values from 9 to 15 kW.

For many melt runs severe under-cut at the welt crown, up to 0.5 mm in depth was observed. The most pronounced under-cut was observed for welding velocities of 2.5 m/min and 3.0 m/min, while no significant undercut was reported for 1.5 m/min and 2.0 m/min.

The penetration of the melt runs was measured from etched cross-sections (Figure 5). The penetration increased with laser power and decreased with welding velocity, in line with an increase in heat input (Figure 6). The dominant microstructure within the weld fusion zone was a columnar dendritic structure (Figure 7). The structure generally was very fine compared to higher heat input processes due to the rapid solidification and cooling rates but similar to structures reported by Yan et al. (2010) for CO_2 laser welding of 3mm thick 304L plates. All of the welds displayed a centreline grain boundary with the dendritic grain growth from the fusion zone interface towards the weld centreline (Figure 5). The phases present in the microstructure are delta ferrite at the dendritic boundaries and austenite islands adjacent, as predicted in the literature by Kotecki and Siewert (1992) and later in more detail by Kyriakongonas (2008). The morphology of the delta ferrite is predominantly skeletal, however there are areas that show features of lathy ferrite.

No clear indication for a HAZ was discerned suggesting that it is very small and can not be resolved from the fusion zone. The HAZ in austenitic steel is related to grain growth and not to phase transformations. Considering the high velocity and the localized heat input of the laser welding process there was insufficient time available for the development of an extensive HAZ.
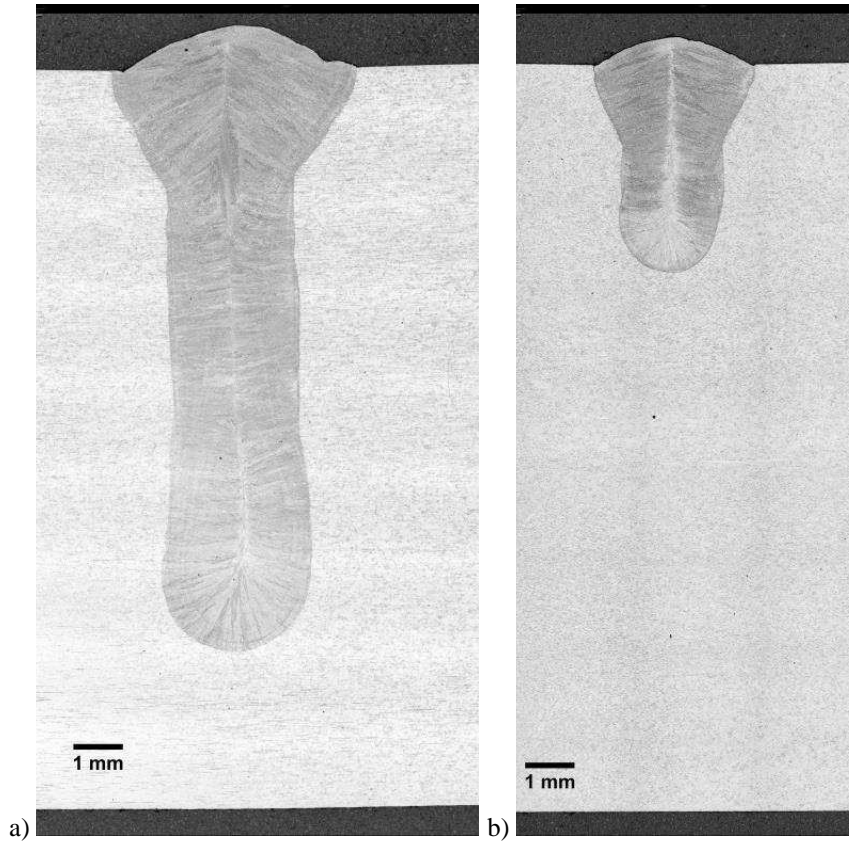
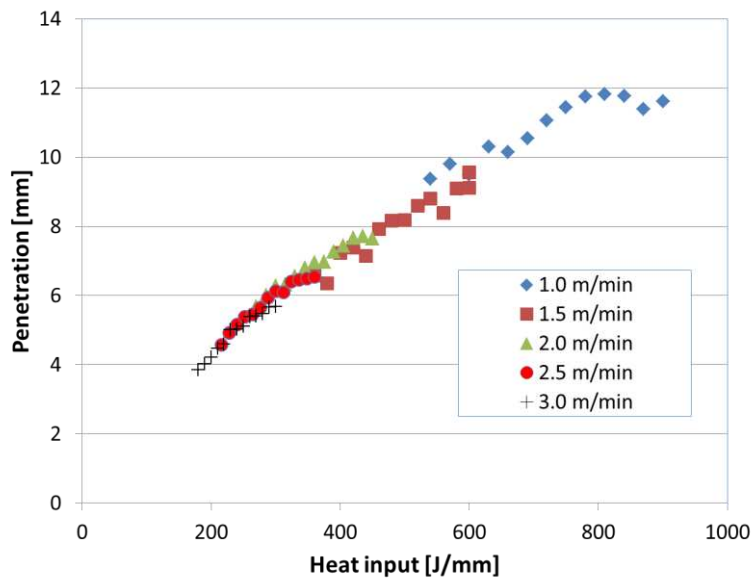**Figure 5 Etched cross sections of melt runs: a) P = 14.0kW, v = 1.0m/min, b) P = 10.0kW v = 3.0m/min**

Figure 6 Penetration depth of the melt runs in dependence of the heat input

8

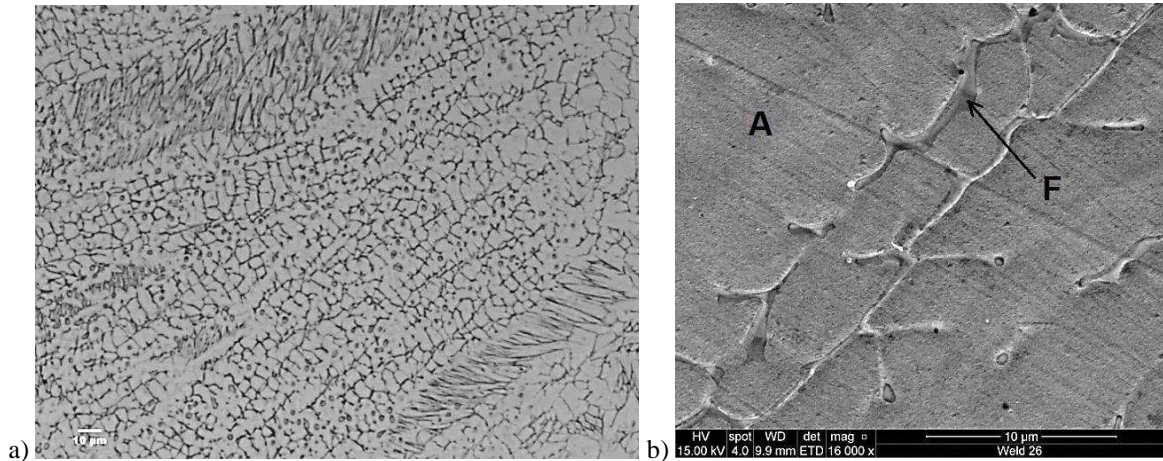**Figure 7 a) Lathy and skeletal ferrite morphologies (P = 12 kW, v = 2.5 m/min), b) austenite (A) and delta ferrite phase (F) (P = 12 kW, v = 1.5 m/min)**

For many of the melt runs no internal defects were observed. For about 1/5 of all melt runs however defects like solidification cracks with occasional intergranular branching off and pores, both in the centre line were reported. Almost exclusively these defect types were observed for melt runs at 1 m/min and all of them for melt runs at high heat input.

The dendritic boundaries (Figure 7b) displayed a significant increase in chromium of up to 24 wt.% compared to 19 wt.% and a decrease in nickel to roughly half of that of the austenitic matrix. This supports the presence of delta-ferrite at the dendritic boundaries because chromium is a ferrite stabiliser with nickel being an austenite stabiliser as indicated by Lampman (1997).

Measurements of the solidification grain and subgrain size within the weld were done using the ASTM E112-13 Line Intercept method. The cell diameter increased with heat input (Figure 8). The cell size generally decreased from the top towards the bottom of the weld.
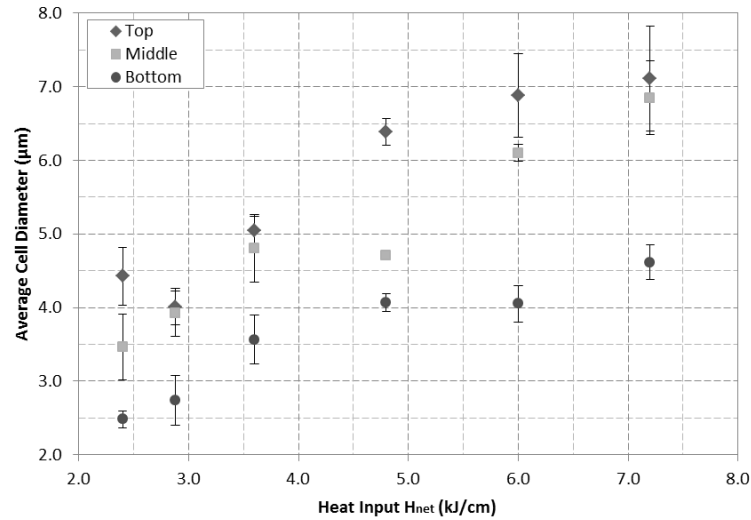
Figure 8 Average cell diameter within the weld at the top, middle and bottom of the weld as a function of the heat input for variations of the welding velocity from 1 to 3 m/min and a laser power of 12 kW and for variations of the laser power from 9 to 15 kW at a welding velocity of 1.5 m/min

Micro-Vickers-hardness measurements across the fusion zone revealed locally strong variations in hardness. The average value increased with the welding velocity (Figure 9). The increased welding velocity at constant laser power translates into a decrease in heat input. The increasing hardness with decreasing heat input may attributed to smaller grain sizes (Figure 8) which is potentially related to faster cooling rates. It is noteworthy that the hardness values in the fusion zone were similar to the values of the base materials.
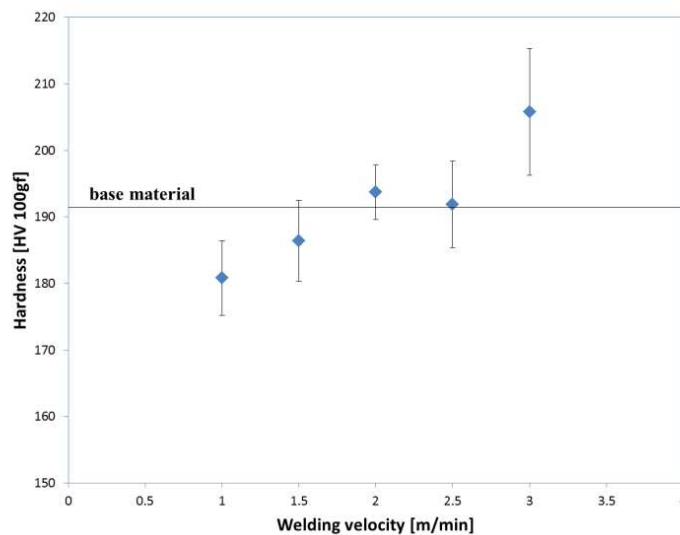

Figure 9 Average hardness in the middle of the fusion zone for melt runs at 12 kW in dependence on the welding velocity. The average value for the base material is given as comparison.

Results of butt welding

The analysis of the melt runs has shown the tendency of the formation of internal defects at high heat input (especially at 1.0 m/min) and the development of extensive sinking at the crowns for high welding velocities. In order to achieve good butt welding of 10 mm thick plates, the welding velocity was chosen to be 1.5 m/min.

Butt welding experiments indicated that less heat input is required to achieve the same penetration than for the melt runs. At a velocity of 1.5 m/min and a laser power of 12 kW, 10 mm thick plates were fused together while for melt runs at the same parameter set only 8 mm penetration was achieved. A well-developed crown and root were achieved for the entire length of the weld. The crown was oxidised and the root remained shiny indicating a different quality of shielding gas protection at the crown and the root. The crown was relatively flat with an inclination to limited sinking at the end of the weld. Compared to the crown the root was very pronounced (Figure 10). The microstructure of the butt weld was similar to the one described for the melt runs. No cracks were found in any of three cross-sections of this weld; however a small amount of porosity was observed at random locations. The maximum pore diameter was 54 μm which is within the acceptance criteria of ASME VIII Division 1 standards ASME (2013).
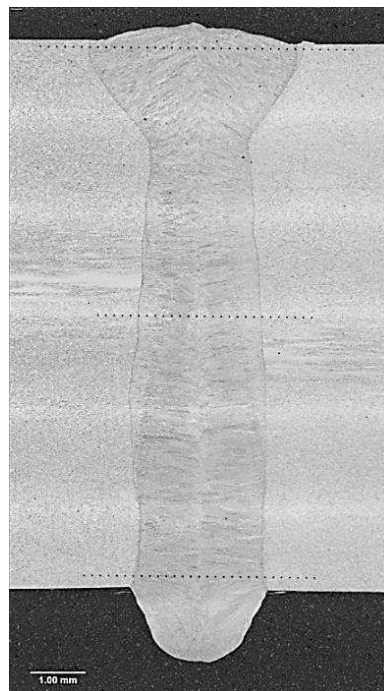

Figure 10 Cross-section of the butt weld including three indentation lines for hardness (viewed towards the end of the weld run)

11

The hardness measurements (three indentation lines clearly visible in Figure 10) have resulted to values averaged 190 HV100gf for all three measurements of the fusion zone (Figure 11), which is in agreement with the results from the melt runs. No extensive hardening of the fusion zone compared to the base material was observed. The hardness of the base material was around 190 HV100gf in the case of measurements in the middle and bottom region (Figure 11b and c), However in the case of the area near the crown the base material hardness is significantly higher (Figure 11a),
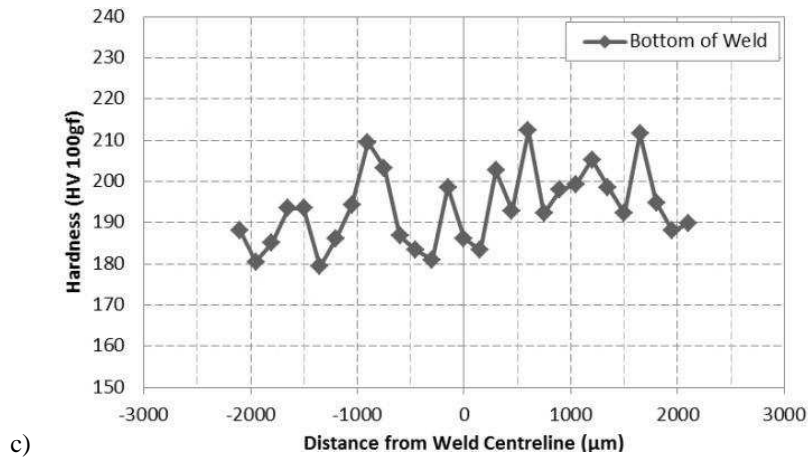

a)

b)

c)
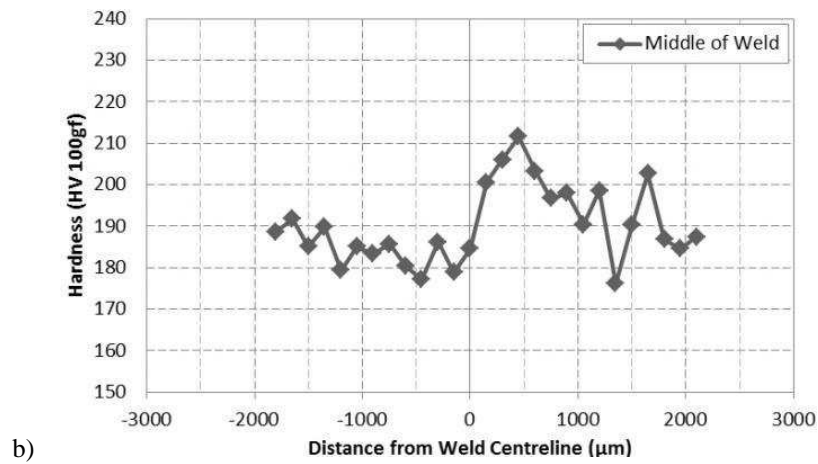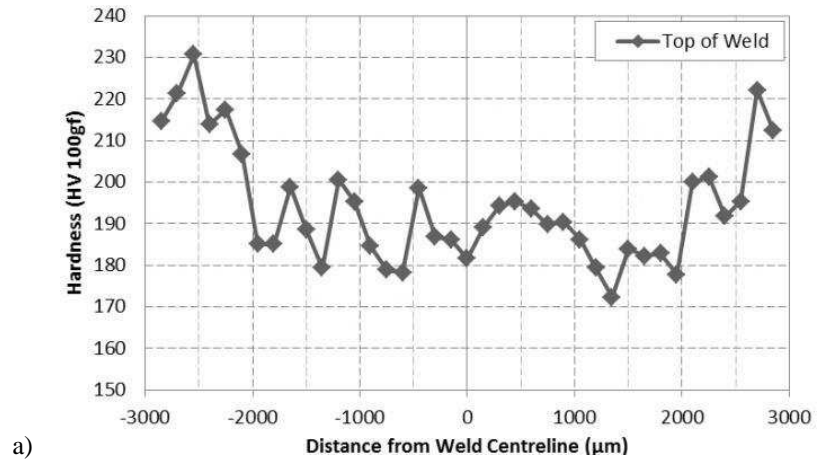
Figure 11 Hardness measurements plotted against the distance from the weld centreline for the butt weld produced at *P*=12kW and *v*= 1.5m/min in locations a) top b) middle and c) bottom in the weld FZ.

Discussion

As Hemmerich et al. (2014) have pointed out focus shift in laser materials processing optics is a major source of disturbance when using high-power laser sources of increased beam quality and strong focusability. They have described that with the absorption of laser power in the beam forming optics. This means for the present set-up that with increasing operational laser power more energy is absorbed. This leads to a significant loss in power efficiency and to a power dependent focus shift (Figure 2). Such power dependent focus shift had also been reported by Reitemeyer et al. (2010) who have attributed 59% of a focus shift over 7 kW to the process optics while the rest derived from beam source, fibre and measuring devise. It is noted that the laser beam of the present set-up had a large divergence and a relatively small Rayleigh length. The focal shift at nominal 15 kW is about 27% of the Rayleigh length. This means it is imperative to know the working distance and focus shift accurately in order to achieve optimal results.

While the laser power dependency of focus shift and power efficiency were significant the changes in Rayleigh length and focus diameter (Figure 3) were marginal and close or within the measurement errors and can be neglected.

Key process parameters in laser welding are laser power P, welding velocity *v* and beam diameter *d*. Figure 6 shows a clear relationship between heat input and penetration allowing a good prediction for the present set-up for different laser power and velocity combinations. However a direct application of this correlation for other optical set-ups with different beam diameters is not possible. It was shown by Suder and Williams (2014) that the heat input alone can not describe performance since the beam diameter is not considered. Nevertheless they have claimed that

13

certain combinations of all three parameters may lead to welds with similar penetration depth. To achieve that Suder and Williams (2014) have introduced the power factor P_F and interaction time τ_i:

$$P_F = \frac{P}{d}$$

$$\tau_i = \frac{d}{v}$$

They have claimed that an unique relation $P_F(\tau_i)$ exists to achieve a specific penetration for a certain material. According to them one could achieve the same melt run penetration for different beam diameters just by determining the required laser power and welding velocity from this relation. Suder and Williams (2014) have presented their results for a fibre laser with a maximum output of 8 kW, a beam diameters between 0.38 and 0.78 mm, and low carbon steel S355. These conditions were therefore very different to the present paper. Figure 12 is a plot of the power factor over the interaction time of selected welds with measured penetration of approximately 4 mm, 6 mm and 8 mm in comparison to the results by Suder and Williams (2014). While only the result for 8 mm coincided with the predicted curves the other results followed generally the trend. The deviation may be contributed to inaccuracies in measurements and to the differences in material. Further work investigating this theory by varying the optical set-up is planned.
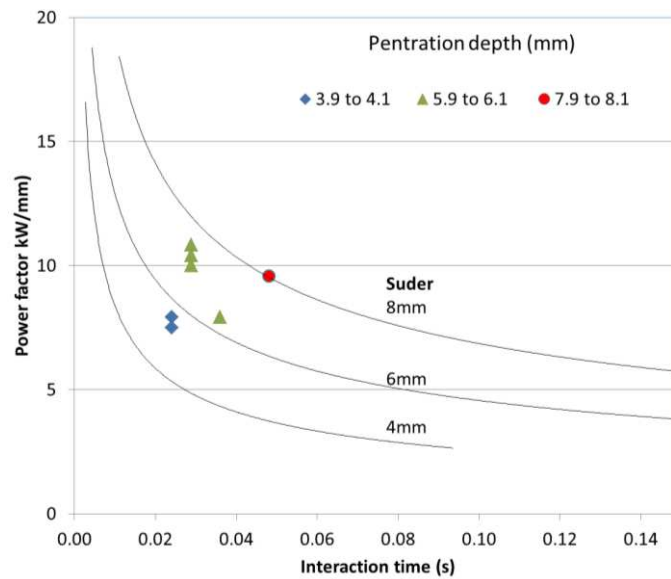
Figure 12 Power factor and interaction time calculated for welds with penetration of approximately 4 mm, 6 mm and 8 mm compared to relations predicted by Suder and Williams (2014).

It was observed that certain sets of welding parameters have resulted in defects like cracks and undercut at the crowns. Stainless steel 304L is susceptible to centre line welding cracks as described by Lippold (1985). In the present work they were related to a low welding velocity and a high heat input which coincides with the largest weld widths (Figure 4). It is believed that in these cases the material was more prone to cracking since at slower speed the weld is wider and higher stresses develop due to larger transvers shrinkage during weld pool solidification. The undercut in the case of high velocities was the result for not allowing enough time for the weld bead to wet the edges of the plate and pulling too much molten material into the middle creating a pronounced convex weld crown.

The reported morphology in the fusion zone consisted of austenite with a small percentage of delta-ferrite at the dendrite boundaries. A directional nature of the microstructure around the axis of the laser beam has been observed which is in accordance with El-Batahgy (2012). A refinement of the dendritic structure by increasing the welding speed at constant power was observed. Similarly a finer structure developed for lower laser powers at constant velocity. The cell size generally decreased from the top towards the bottom of the weld. This change in microstructure could be attributed to the increase in the cooling and solidification rates with decreasing heat input, respectively from top to bottom. The refinement of the microstructure with increasing welding velocity was reflected by an increased hardness.

15

It is worthwhile to note that the hardness in the fusion zone is comparable to the values for most of the substrate areas. Only for the measurements of the base material one of the surfaces (next to the crown) higher values of up to 230 HV100gf were reported. This hardening of the surface of the base material may be attributed to work hardening either during the rolling process of the manufacture of the plates or during surface machining.

Conclusion

The analysis of the diode laser beam indicated that for the range between 1 kW and 15 kW the minimum beam diameter was 1.2 mm and the Rayleigh length between 4 mm and 3.2 mm. The focus shifted linearly with the power by less than 1 mm. The effective laser power decreased with the nominal laser power to 89% at 15 kW.

Melt runs on stainless steel plates of 304L were performed. A wide range of laser power from 9 kW to 15 kW and welding velocities from 1 m/min to 3 m/min demonstrated a clear dependence of the penetration on the heat input. At the maximum heat input a penetration of 12 mm was achieved.

Melt runs at high heat input, especially at a low welding velocity of 1.0 m/min, were prone to defects including solidification cracking in the centre and small pores. High welding velocities of 2.5 m/min and 3.0 m/min resulted in significant sinking at the crowns. These observations and the aim to achieve butt welds of 10 mm have narrowed down potential parameter sets. A parameter set with a welding velocity of 1.5 m/min and a laser power of 12 kW was judged to be the optimum for fusion welding of 10 mm thick plates.

It may be concluded that high powered diode lasers are capable of deep penetration welding applications. Keyhole mode welding was achieved and the weld properties are comparable to that of other high energy density welding processes. For welding of plates in the 10mm thickness range, the results suggest that the more economic diode laser systems may become a competitor to other systems with high quality laser beams which may be more expensive in both procurement and operation.

References

ASME, 2013. ASME Boiler & Pressure Vessel Code, VIII Rules for construction of pressure vessels, Division 1, New York.

Baufeld, B., Lawler, S., 2016. Laser Cladding of Large Scale Parts at the Nuclear AMRC, 9th International Laser Symposium, Dresden.

Baufeld, B., Lawler, S., Hillig, H., Bridger, K., 2014. Diode laser cladding for large surface areas, International Laser Symposium "Fibre, Disc, Diode", Dresden, Germany.

Buddu, R.K., Chauhan, N., Raole, P.M., Natu, H., 2015. Studies on mechanical properties, microstructure and fracture morphology details of laser beam welded thick SS304L plates for fusion reactor applications. Fusion Engineering and Design 95, 34-43.

Bush, S.H., 1990. The Effects of Erosion-Corrosion on Power Plant Piping, 59th General Meeting of the National Board of Boiler and Pressure Vessel Inspectors.

Dausinger, F., 2000. Laser welding of aluminum alloys: from fundamental investigation to industrial application, In: Chen, X., Fujioka, T., Matsuanwa, A. (Eds.), High-Power Lasers in Manufacturing. SPIE, Osaka, Japan, pp. 367-379.

De Baglion, L., Mendez, J., 2010. Low cycle fatigue behavior of a type 304L austenitic stainless steel in air or in vacuum, at 20 °C or at 300 °C: Relative effect of strain rate and environment. Procedia Engineering 2, 2171-2179.

El-Batahgy, A.M., 2012. Laser Beam Welding of Austenitic Stainless Steels - Similar Butt and Dissimilar Lap Joints, INTECH, pp. 93-116.

Hemmerich, M., Thiel, C., Lupp, F., Hanebuth, H., Weber, R., Graf, T., 2014. Reduction of Focal Shift Effects in Industrial Laser Beam Welding by Means of Innovative Protection Glass Concept. Physics Procedia 56, 681-688.

Henderson, M.B., Arrell, D., Larsson, R., Heobel, M., Marchant, G., 2004. Nickel based superalloy welding practices for industrial gas turbine applications. Science and Technology of Welding and Joining 9, 13-21.

Kotecki, D.J., Siewert, T.A., 1992. WRC-1992 Constitution Diagram for stainless steel weld metals: a modification of the WRC-1988 Diagram. Welding Journal 71.

Kyriakongonas, A.P., 2008. 3D Numerical Modeling of Austenitic Stainless Steel 316L Multi-pass Butt Welding and comparison with Experimental Results, SCHOOL OF NAVAL ARCHITECTURE AND MARINE ENGINEERING. NATIONAL TECHNICAL UNIVERSITY OF ATHENS, Athens, Greece, p. 119.

Lampman, S., 1997. Weld Integrity and Performance. ASM International.

Lippold, J.C., 1985. Centerline Cracking in Deep Penetration Electron Beam Welds in Type 304L Stainless Steel. Welding Journal 64, 127-136.

Mootz, A., 2016. Application of brilliant laser beam source for powertrain production, International Laser Symposium & International Symposium Tailored Joining, Dresden, Germany.

Neumann, M., 2016. Lasergeschweisste Sonderprofile - Bausteine fuer innovative Leichtbau- und Dickblechloesungen, 10th International Conference Beam Technology, Halle, Germany, pp. 1-4.

Parker, K., 2010. Welding with High power Diode Lasers, http://www.photonics.com/WhitePaper.aspx?WPID=372.

Ready, J.F., 1997. Industrial applications of lasers, 2nd ed. Academic Press.

Reitemeyer, D., Seefeld, T., Vollertsen, F., 2010. Online focus shift measurement in high power fiber laser welding. Physics Procedia 5, 455-463.

Suder, W.J., Williams, S., 2014. Power factor model for selection of welding parameters in CW laser welding. Optics & Laser Technology 56, 223-229.

Ullmann, C., 2014. Are there Limits for multi kW Diode Laser?, International Laser symposium & International Symposium Tailored Joining, Dresden, Germany.

Ullmann, C., 2016. High power diode laser in a balancing act between innovation and production technology, International Laser symposium & International Symposium Tailored Joining, Dresden, Germany.

Yan, J., Gao, M., Zeng, X., 2010. Study on microstructure and mechanical properties of 304 stainless steel joints by TIG, laser and laser-TIG hybrid welding. Optics and Lasers in Engineering 48, 512-517.

Zhang, M., Chen, G., Zhou, Y., Liao, S., 2014. Optimization of deep penetration laser welding of thick stainless steel with a 10 kW fiber laser. Materials & Design 53, 568-576.

19